Advanced Remote Sensing

http://publish.mersin.edu.tr/index.php/arsej

e-ISSN 2979-9104

Evaluation of the relationship between urban area and land surface temperature determined from optical satellite data: A case of Istanbul

Gülcan Sarp*[1], Emre Baydoğan [1], Firdevs Güzel [1], Tuğba Otlukaya [1]

[1]Suleyman Demirel University, Department of Geography, Türkiye, gulcansarp@sdu.edu.tr, emrebay07@gmail.com, firdevsguzel3@gmail.com, tgbkocabas@gmail.com

Cite this study: Sarp, G., Baydoğan, E., Güzel, F., & Otlukaya, T. (2021). Evaluation of the relationship between urban area and land surface temperature determined from optical satellite data: A case of Istanbul. Advanced Remote Sensing, 1(1), 31-37

Keywords
Land Surface Temperature
Normalized Building Difference Index
Landsat 8 OLI-TIRS

Research Article
Received: 16.11.2021
Revised: 12.12.2021
Accepted: 19.12.2021
Published: 30.12.2021

Abstract

In recent years, the formation of urban heat islands occurring both depending on urban structuring and human activities has been the focus of attention of many researchers. In particular, remote sensing data has been widely used in this type of research. Because with the development in satellite and remote sensing technologies, satellite sensors that detect at different spatial, spectral, and radiometric resolutions not only enable the determination of land use classes on the Earth's surface but also allow the determination of the land surface temperature. In this study, Landsat 8 OLI-TIRS images of 2018 were used to determine the urban area and land surface temperature. Urban areas were determined by applying Normalized Building Difference Index (NDBI) to the Short-Wave Infrared (SWIR) and Near Infrared (NIR) bands of the Landsat 8 OLI sensor. Thermal Infrared (TIR) bands of the Landsat 8 TIRS sensor were used to determine the land surface temperature (LST). According to the results obtained, the lowest average temperature value is 22 °C in the Adalar district and the highest average temperature value is 33 °C in the Gaziosmanpaşa district, and there is a positive 76% linear relationship between the urban object ratio and the land surface temperature.

1. Introduction

It is known that urban areas with dense impermeable surfaces such as buildings or roads have an impact on climate at different scales. Therefore, urban areas tend to offer a higher temperature compared to the surrounding rural areas.

Today, the increasing availability of images from Landsat series satellites on a global scale has enabled both periodic and high spatial resolution analysis of the relationship between urban growth dynamics and land surface temperature. To make this comparison correctly, first of all, it is necessary to determine the urban areas from satellite images with high spatial accuracy. For this purpose, different algorithms designed to determine urban areas with high spatial accuracy have been proposed in the literature. Some of those; Urban Index (UI) [1], Bare soil index (BI) [2], Normalized Difference Bareness Index (NDBaI) [3], Index-based building index (IBI) developed to determine the characteristics of built-up areas from satellite images [4], and Enhanced Built-Up and Bareness Index (EBBI) developed to map built-up and bare land in an urban and urban area [5], have been employed in various studies. These indices are widely adopted for monitoring urban growth, given their relative simplicity and easy implementation. The basis of these algorithms is that urban areas have a higher reflection response in the short wavelength infrared (SWIR) wavelength range of the Electromagnetic spectrum compared to green, red, and, near-infrared (NIR) ranges.

Land Surface Temperature (LST) is widely used in hydrology, meteorology, geography, urban heat islands, forest fires, hydrological modeling on a regional and global scale [6-7]. In studies conducted to determine land surface temperature and urban heat island formations. With the developments in remote sensing technologies, satellite sensors that detect in the thermal infrared region of the electromagnetic spectrum are used as an information source for determining the surface temperature. Landsat series satellites of them are often preferred among researchers because they have sensors that shoot in the Thermal Infrared (TIR) region. Taha [8] determined the causes and effects of the formation of urban heat islands. Jiang and Tian [9], on the other hand, investigated the effects of land change and land use on land surface temperature using the thermal bands of Landsat ETM+ satellite imagery. Bokaie et al. [10] evaluated the urban heat island in Tehran based on the relationship between land use and land surface temperature. Sarp [11] investigated the relation between LST and vegetation relation based on Landsat TM5 data and found a significant inverse relationship between the LST and vegetation. Erener and Sarp [12] evaluated the environmental effects of the dams in their study and tested the relationship between vegetation, surface humidity, and surface temperature distributions in these areas statistically. Sarp et al. [13] evaluated industrialization effects on urbanization and urban heat island formation and found a strong relationship between industrialization, urbanization, and heat island formation. Zhang et al. [14] evaluated the changes in LST of the Ebinur lake between 1998 and 2011 and stated that the Landsat image is valuable data to estimate the relationship between LST and land cover factors. Temurçin et al. [15] evaluated the urban heat island formations through the structural differences in the morphology of the Istanbul city. In the study, they observed that the urban heat island effects increase in areas with high building density in the horizontal and vertical directions and that the urban heat island values increase by 1-2 °C in areas where the vertical structuring is intense compared to the surrounding areas.

In this study, the relationship between land surface temperature and urban areas obtained from Landsat 8 OLI (Operational Land Imager) and TIRS (Thermal Infrared Sensor) satellite images were tried to be evaluated for the province of Istanbul. The difference of this study from previous studies is the use of images from the same satellite in determining both urban areas and land surface temperature, as well as a statistical comparison of urban object density and land surface temperature values on a district basis.

2. Material and Method

The image of the Landsat 8 OLI-TIRS satellite was used in the study, dated April 23, 2018, was downloaded free of charge from the United States Geological Survey (USGS) website [16]. Landsat 8 satellite has 2 sensors, OLI and TIRS. This satellite receives images in the Visible, Near Infrared (NIR), Short Wave Infrared (SWIR) and Thermal Infrared (TIR) ranges and has a spatial resolution of between 15 and 100 meters depending on the spectral range [7]. The technical specifications of the Landsat 8 OLI- TIRS satellite are given in Table 1 [7].

Table 1. Technical Specifications of Landsat 8 OLITIRS satellite

Bands	Spectral Range (micrometers)	Resolutions (m)
Band 1 Costal Aerosol	0.43 - 0.45	30
Band 2 Blue	0.45 - 0.51	30
Band 3 Green	0.53 – 0.59	30
Band 4 Red	0.64 – 0.67	30
Band 5 Near InfraRed	0.85 – 0.88	30
Band 6 Short Wave Infrared (SWIR1)	1.57 – 1.65	30
Band 7 Short Wave Infrared (SWIR2)	2.11 – 2.29	30
Band 8 Panchromatic	0.50 – 0.68	15
Band 9 Cirrus	1.36 – 1.38	30
Band 10 Thermal Infrared	10.60–11.19	100
Band 11 Thermal Infrared	11.50 – 12.51	100

The method of the study consists of four different stages. In the first stage, Normalized Building Difference Index (NDBI) was obtained from the SWIR and NIR bands of the Landsat 8 OLI sensor, and the Normalized Vegetation Difference Index (NDVI) was obtained from the NIR and R bands of the Landsat 8 OLI sensor. In the second stage, NDBI and NDVI imageries are converted to binary classes with the help of natural breaks Jenks algorithm. In the third stage, the Land Surface Temperature (LST) was obtained from the TIR (band 10) of the Landsat 8 TIRS sensor. In the last stage, the relationship between the urban object ratios in each district area and the LST was evaluated with the Pearson linear correlation.

2.1. Normalized Difference Built-Up Index (NDBI)

For the identification of urban areas from Landsat 8 OLI-TIRS satellite images, Normalized Building Difference Index (NDBI) proposed by Zha et al. [17] was used. The main purpose of developing this index is to highlight urban areas with higher reflectance in the short-wave infrared (SWIR) region and lower in the near-infrared (NIR) region. NDBI is calculated using the Equation 1.

$$NDBI=((SWIR-NIR))/((SWIR+NIR)) \quad (1)$$

In the resulting image (Figure 1a), NDBI values vary between -1 and +1, values close to +1 correspond to areas with urban objects (buildings, roads, etc.), while values close to -1 correspond to green areas and soil areas where there is no settlement.

Since only urban objects are dealt with in this study, NDBI results are converted into binary classes representing residential areas (1) and other areas (0) with the natural breaks Jenks algorithm (Figure 1b). In the resulting image, residential areas representing urban objects could be determined up to 30 m in spatial resolution provided by Landsat 8 OLI satellite.

To determine the urban object ratio on a district basis, the urban object ratios were calculated by districts, taking into account the number of values represented by 0 and 1 within each district boundary (Table 2). According to the results obtained, the districts with the highest rate of urban objects are Güngören with 52%, Gaziosmanpaşa with 45%, and Şişli with 42%. The districts with the lowest rate of urban objects are Şile with 2%, Çekmeköy, Adalar, and Beykoz districts with 3%.

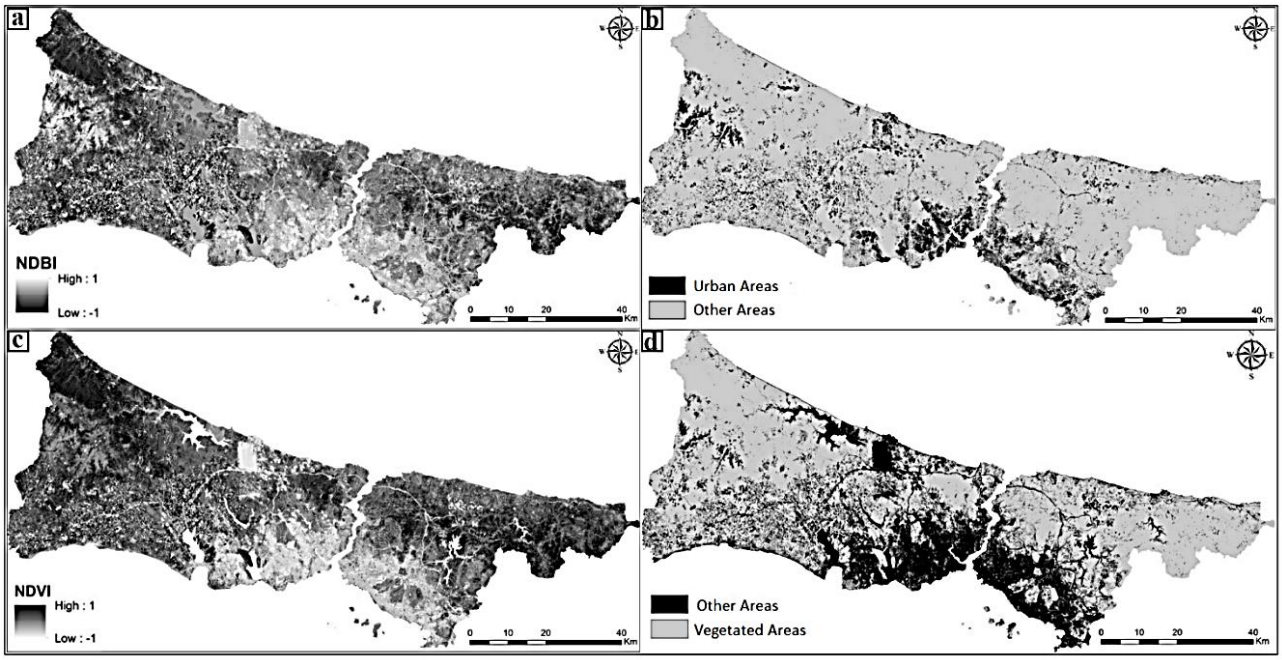

Figure 1. Normalized Building Difference Index (NDBI) Result **(a);** The result of the Jenks algorithm applied to the NDBI (0 (other areas) and 1 (urban areas)) **(b);** Normalized Difference Vegetation Index (NDVI) Result **(c);** The result of the Jenks algorithm applied to the NDVI (0 (other areas) and 1 (vegetated areas)) **(d).**

Table 2. Urban object ratios by districts

District Name	Building Density by Districts (%)	District Name	Building Density by Districts (%)
Şile	2	Çekmeköy	3
Bağcilar	31	Güngören	52
Kağithane	24	Arnavutköy	6
Beşiktaş	17	Esenler	24
Fatih	39	Zeytinburnu	29
Kadiköy	30	Ümraniye	24
Küçükçekmece	15	Sultanbeyli	20
Adalar	3	Bahçelievler	38
Esenyurt	21	Sultangazi	12
Gaziosmanpaşa	45	Sariyer	4
Bakirköy	13	Tuzla	8
Beylikdüzü	8	Ataşehir	22
Bayrampaşa	29	Başakşehir	6
Büyükçekmece	7	Beykoz	3
Eyüpsultan	5	Sancaktepe	10
Şişli	42	Avcilar	14
Üsküdar	22	Silivri	8
Kartal	20	Maltepe	14
Beyoğlu	40	Pendik	9
Çatalca	4		

2.2. Normalized Difference Vegetation Index (NDVI)

The NDVI index is a measure of the amount and vitality of surface vegetation. Considering that green vegetation containing chlorophyll reflects well in the near-infrared (NIR) part of the spectrum and absorbs well in the red (R) wavelength range in the visible region, the NDVI is calculated using Equation 2 [18].

$$\text{NDVI}=(\text{NIR-R})/(\text{NIR+R}) \tag{2}$$

The NDVI result obtained is presented in Figure 1c. In this figure, NDVI values vary between -1 and +1, and values close to +1 represent areas with active vegetation and low (near-zero or negative) values indicate other types of materials [19]. To determine only the green areas from the NDVI image, the natural breaks Jenks algorithm was applied to the NDVI results. The resulted binary images indicating 0 (other areas) and 1 (vegetated areas) were given in Figure 1d.

2.3. Land Surface Temperature (LST)

The thermal band (Band 10) of the TIRS sensors of the Landsat 8 satellite was used to obtain the LST values. For the LST analysis, firstly, the numerical values (DN) were converted into spectral reflectance values using Equation 3 (4).

$$L\lambda = \frac{(LMAX\lambda - \text{LMİN}\lambda)}{(QCALMAX\lambda - \text{QCALMİN}\lambda)} x\ (DN - QCalmin) + LMin\lambda \tag{3}$$

In this formula; Lλ shows the spectral radiance value, DN shows the numerical cell values, Lmin and Lmax show the minimum and maximum spectral reflectance values in the thermal band, QCalMin, and QCalMax show the calibrated minimum and maximum cell values [20]. Equation 4 was used to convert the obtained spectral reflectance values to temperature values.

$$T = \frac{K_2}{\ln\left(\frac{K_1}{L_\lambda}\right) + 1} \tag{4}$$

where, T represents the temperature value in Kelvin, and K1 and K2 are the calibration constants of the TIR band. In this case, K1 and K2 constants for the Landsat 8 TIR band 10 are 774.89 and 480.89, respectively.

The obtained land surface temperature distribution is shown in Figure 2. In this figure, the temperature distributions in the study area vary between 12.77 ^{0}C and 48.67 ^{0}C. Areas with high temperatures generally correspond to areas with dense urban objects, while areas with low land surface temperature generally correspond to wetlands and green areas obtained as a result of NDVI.

Considering the averages of LST values on a district basis (Table 3), it was determined that the lowest average temperature value was 22 ^{0}C in the Adalar district and the highest average temperature value was 33 ^{0}C in Gaziosmanpaşa district.

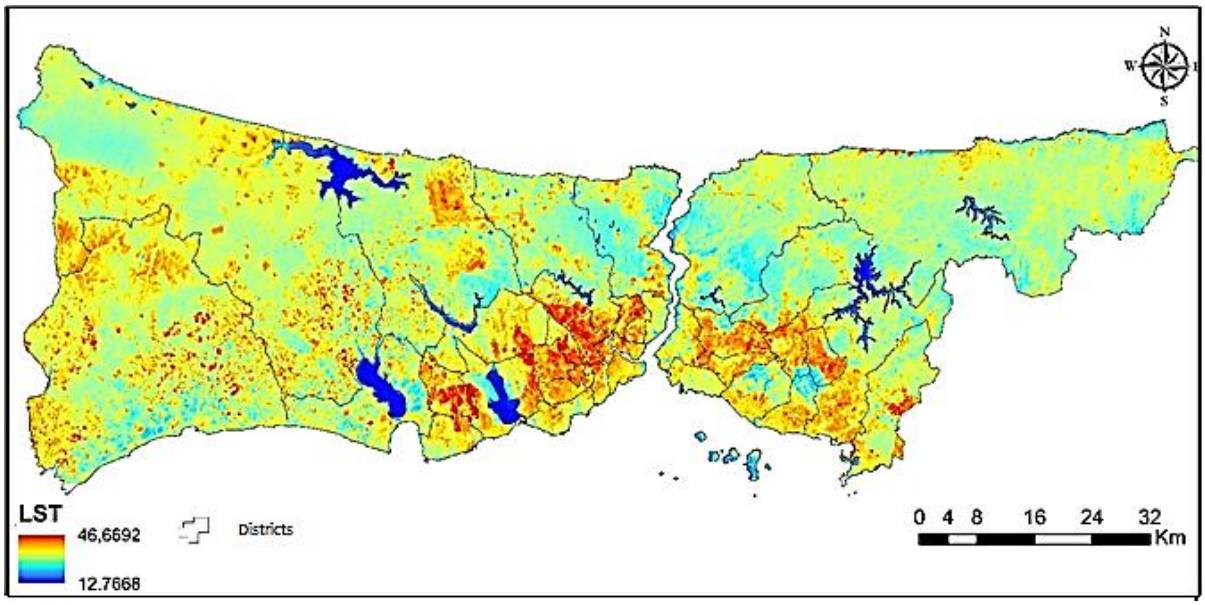

Figure 2. Land Surface Temperature Map (LST)

Table 3. Descriptive statistics of Land Surface Temperature (LST) by districts

District Name	Min (°C)	Max (°C)	Mean (°C)	District Name	Min (°C)	Max (°C)	Mean (°C)
Şile	16	37	26	Çekmeköy	17	36	26
Bağcilar	25	39	31	Güngören	27	35	31
Kağithane	24	36	31	Arnavutköy	15	47	27
Beşiktaş	16	33	27	Esenler	24	36	30
Fatih	16	35	29	Zeytinburnu	18	36	29
Kadiköy	15	38	28	Ümraniye	22	43	30
Küçükçekmece	17	39	29	Sultanbeyli	21	36	30
Adalar	16	30	22	Bahçelievler	24	38	30
Esenyurt	23	44	31	Sultangazi	19	37	29
Gaziosmanpaşa	26	37	33	Sariyer	14	37	26
Bakirköy	17	42	28	Tuzla	17	41	28
Beylikdüzü	17	41	28	Ataşehir	22	44	30
Bayrampaşa	25	46	32	Başakşehir	21	41	28
Büyükçekmece	17	42	27	Beykoz	14	36	26
Eyüpsultan	18	38	27	Sancaktepe	19	35	28
Şişli	24	35	30	Avcilar	18	37	28
Üsküdar	17	34	28	Silivri	17	45	28
Kartal	18	38	28	Maltepe	20	36	27
Beyoğlu	14	35	30	Pendik	17	40	27
Çatalca	16	38	27				

2.4. Evaluation of the relationship between land surface temperature and urban object ratio with pearson linear correlation

Correlation is a measure of the relationship between two variables. A change in the size of one variable in related data is related to the size of another variable in the same or opposite direction. This relationship value can vary between -1 and +1. Values close to -1 mean that the relationship is negative, and values close to +1 mean that the relationship is strong and positive [21].

The relationship between the two variables is determined by the Pearson Linear Correlation coefficient [22]. This correlation coefficient was developed by Karl Pearson (1857–1936). The Linear Correlation coefficient is given in Equation 5 [23].

$$r = \frac{n(\sum xy) - (\sum x)(\sum y)}{\sqrt{[n\sum x^2 - (\sum x)^2][n\sum y^2 - (\sum y)^2]}} \quad (5)$$

Where r is the Pearson Coefficient, ∑xy is the sum of the product of the paired data, ∑x and ∑y are the sums of data, $\sum x^2$ and $\sum y^2$ are the sums of the squares of the data.

In this study, the averages of the land surface temperatures obtained in the districts and the percentage distributions of the urban object ratios in the districts were evaluated with the Pearson linear correlation method. According to the results obtained, the r value is 0.76. This value indicates that there is a positive relationship between these two variables.

3. Results and Discussions

As a result of the study, the building densities falling within each district boundary and the temperature values within the district boundaries were compared. According to the districts, the average surface temperature is the lowest at 22 °C, and the highest temperature is 33 °C. The district with the lowest temperature is Adalar, and the district with the highest temperature is Gaziosmanpaşa. When we look at the urban object ratios of the districts, the highest urban object ratio is Güngören district with 52%. The district with the lowest rate of urban objects is Şile with 2%.

The positive linear relationship between urban object ratios and surface temperatures is 76%. When the NDVI results are compared with the LST distributions, it is observed that the LST distributions show high values not only in urban areas but also in bare lands [24]. Urban areas, pavements, asphalt, buildings, etc., absorb and retain heat. surfaces are exposed to higher temperatures due to one reason for having high-temperature values for bare land is that most bare areas are devoid of vegetation. This leads to an increase in the amount of thermal energy emitted by the bare ground and hence an increase in temperature [24]. Green areas in urban areas have a positive effect on land surface temperature in terms of reducing the effect of urban heat island formation. Especially in these areas, the cooling effect through shadow and evaporation helps to regulate the urban climate and reduce the effect of the urban heat island [13,25]. In the study, urban and vegetated areas were extracted from 30 m resolution

bands. On the other hand, LST was extracted from a 100 m resolution thermal band. Therefore, the comparison was made with air temperature, which is different and can sometimes result in big differences [26]. Rapid changes in environment may adversely affect ecosystem [27]. As a result, the increase in vegetation and wetlands caused a decrease in LST values, while the building density in urban areas caused an increase in LST values and vice versa [14]. In the study, this situation was also confirmed by Pearson Linear Correlation.

4. Conclusion

This study described the relationship between land surface temperature and urban area, in Istanbul which is a densely urbanized city of Turkey. In the study urbanization density and LST are taken into account at the district base and the building densities falling within each district boundary and the temperature values within the district boundaries were compared. According to the districts, the average surface temperature is the lowest at 22 °C, and the highest temperature is 33 °C. The district with the lowest temperature is Adalar, and the district with the highest temperature is Gaziosmanpaşa. When we look at the urban object ratios of the districts, the highest urban object ratio is Güngören district with 52%. The district with the lowest rate of urban objects is Şile with 2%.

The comparison reveals that, the positive linear relationship between urban object ratios and surface temperatures, which amount is 76%. On the other hand, the spatial comparison of vegetation areas and urban areas with the LST distributions revealed that the LST distributions show higher temperature values in both urban and bare land.

Funding

This research received no external funding.

Author contributions

Gülcan Sarp: Data curation, Writing-Original draft preparation, Software, Validation, Writing-Reviewing, and Editing. **Emre Baydoğan:** Methodology, Software, Data Analysis, Visualization. **Firdevs Güzel:** Data Preparation, Literature Survey. **Tuğba Otlukaya** Formatting, and Literature Survey.

Conflicts of interest

The authors declare no conflicts of interest.

References

1. Kawamura, M., Jayamana. S., Tsujiko, Y. (1996). Relation between social and environmental conditions in Colombo Sri Lanka and the urban index estimated by satellite remote sensing data. Int. Arch. Photogramm. Remote Sens., 31 (Part B7), 321–326.
2. Rikimaru, A., Miyatake, S. (1997). Development of Forest Canopy Density Mapping and Monitoring Model using Indices of Vegetation, Bare soil and Shadow. In Proceeding of the 18th Asian Conference on Remote Sensing (ACRS) 1997, Kuala Lumpur, Malaysia, 20–25 October 1997; p. 3.
3. Zhao, H.M., Chen, X.L. (2005). Use of Normalized Difference Bareness Index in Quickly Mapping Bare Areas from TM/ETM+. In Proceedings of 2005 IEEE International Geoscience and Remote Sensing Symposium, Seoul, Korea, 25–29 July 2005; 3, 1666–1668.
4. Xu, H. (2008). A new index for delineating built-up land features in satellite imagery. Int. J. Remote Sens. 29, 4269–4276.
5. Assayakur, R., Adnyana, S., Arthana, W., Nuarsa, W. (2012). Enhanced Built-Up and Bareness Index (EBBI) for Mapping Built-Up and Bare Land in an Urban Area. Remote Sensing, 2957-2970.
6. Meng, X., Cheng J., Zhao, S., Liu S., Yao, Y. (2019). Estimating Land Surface Temperature from Landsat-8 Data using the NOAA JPSS Enterprise Algorithm. Remote Sensing, 11, 155.
7. USGS (2021). https://www.usgs.gov/core-sciencesystems/nli/landsat/using-usgs-landsat-level-1-data-product.
8. Taha, H. (2004). Heat Islands and Energy. Encyclopedia of Energy, 133-143.
9. Jiang, J., Tian, G. (2010). Analysis of the impact of Land use/Land cover change on Land Surface Temperature with Remote Sensing. Procedia Environmental Sciences 2, 571-575.

10. Bokaie M., Zarkesh M., Arasteh P., Hosseini A. (2016). Assessment of Urban Heat Island Based on the Relationship between Land Surface Temperature and Land Use/Land Cover in Tehran. Sustainable Cities and Society,94-104.
11. Sarp, G. (2016). Evaluation of Land Surface Temperature and Vegetation Relation Based on Landsat TM5 Data. SCIREA Journal of Geosciences.,1, 1-11.
12. Erener, A. & Sarp, G. (2017). Barajların Çevresel Etkilerinin Zamansal Ve Mekansal Olarak Uzaktan Algılama İle Değerlendirilmesi: Atatürk Barajı Örneği. Geomatik, 2 (1), 1-10. DOI: 10.29128/geomatik.300012
13. Sarp, G., Temurcin, K., Aldirmaz, Y. (2018). Evaluation of Industrialization Effects on Urbanization and Heat Island Formation Using Remote Sensing Technologies: A Case of Istanbul Bağcılar District. Sdü Fen-Edebiyat Fakültesi Sosyal Bilimler Dergisi, 6.
14. Zhang, F., Kung, H., Johnson, V. C, LaGrone B. I., and Wang J. (2018). Change detection of land surface temperature (LST) and some related parameters using Landsat image: a case study of the Ebinur lake watershed, Xinjiang, China. Wetlands, 38 (1), 65–80.
15. Temurçin, K., Sarp, G., Aldırmaz, Y., Kılıç, M. (2019). Şehirleşme İle Kentsel Isi Adası Oluşumu Arasindaki İlişkinin Jeoinformasyon Teknikleri İle Değerlendirilmesi: İstanbul Örneği. Bilge Kağan 2 nd International Science Congress, Bilge Kağan ISC – 2019, 05-06-07 November 2019 Barcelona SPAIN.
16. https://earthexplorer.usgs.gov/
17. Zha, Y., Gao, J., Ni, S. (2003.) Use of normalized difference built-up index in automatically mapping urban areas from TM imagery. International Journal of Remote Sensing, 583-594.
18. USGIS (2022). https://www.usgs.gov/landsat-missions/landsat-normalized-difference-vegetation-index
19. Sarp, G. (2012). Determination of Vegetation Change Using Thematic Mapper Imagery in Afşin-Elbistan Lignite Basin; SE Turkey. Procedia Technology, 1, 407 – 411.
20. Chander, G., and Markham, B. (2003). Revised Landsat-5 TM Radiometric Calibration Procedures and Post Calibration Dynamic Ranges. IEEE Transactions on Geoscience and Remote Sensing. 41 (11), 2674-2677.
21. Schober, P., Boer, C., Schwarte, L.A. (2018). Correlation Coefficients: Appropriate Use and Interpretation. Anesth Analg. 126 (5), 1763-1768. https://doi.org/10.1213/ANE.0000000000002864. PMID: 29481436.
22. Pearson Correlation Coefficient (2021). https://study.com/academy/lesson/pearson-correlation-coefficient-formula-example-significance.html (Last access 23.02.2022)
23. STAT 462; Applied Regression Analysis https://online.stat.psu.edu/stat462/node/96/ (Last access 23.02.2022)
24. Fonseka, H., Zhang, H., Sun, Y., Su, H., Lin., H. L. (2019). Urbanization and Its Impacts on Land Surface Temperature in Colombo Metropolitan Area, Sri Lanka, from 1988 to 2016. Remote sensing, 11(8), 957-975.
25. Gherraz, H., Guechi, I., & Alkama, D. (2020). Quantifying the effects of spatial patterns of green spaces on urban climate and urban heat island in a semi-arid climate." Bulletin de la Société Royale des Sciences de Liège, 89, 164-185.
26. Avdan U., Jovanovska G. (2016). Algorithm for Automated Mapping of Land Surface Temperature Using LANDSAT 8 Satellite Data. Journal of Sensors, 2016, 1480307. https://doi.org/10.1155/2016/1480307
27. Erener, A., & Yakar, M. (2012). Monitoring coastline change using remote sensing and GIS technologies. *Lecture Notes in Information Technology*, *30*, 310-314.